

Volcán de Fuego (Guatemala) monitoring with the Normalized Hotspot Indices (NHI) tool

Nicola Genzano¹, José Armando Saballos^{2,3}, Wendel Gutierrez⁴, Francesco Marchese⁵

¹ Politecnico Milano, Dept. of Architecture, Built Environment and Construction Engineering (DABC) Milano, Italy – nicola.genzano@polimi.it

² University of Edinburgh, UK - j.a.saballos@gmail.com

³ Universidad del Valle, Guatemala

⁴ INSIVUMEH, Guatemala - wagtierrez@insivumeh.gob.gt

⁵ National Research Council, Institute of Methodologies of Environmental Analysis, Tito Scalco (Pz), Italy - francesco.marchese@cnr.it

Keywords: Volcán de Fuego, Normalized Hotspot Indices (NHI) tool, MSI, OLI

Abstract

Volcán de Fuego is a stratovolcano located in Guatemala among the most active in the world. In this work, we investigate its eruptive activity from space by means of the Normalized Hotspot Indices (NHI) algorithm. The latter runs operationally under the Google Earth Engine (GEE) platform providing information on active volcanoes at global scale by means of daytime Sentinel 2 MSI (Multispectral Instrument) and Landsat 8/9 OLI/OLI2 (Operational Land Imager) data. In study, we present the results of a time series analysis performed by investigating 40 years of Landsat observations through the NHI algorithm. Results show that during the major periods of thermal activity (e.g., 2000–2003; 2012–2013; 2015–2018) the Volcán de Fuego generated extended lava flows, which were well identified and mapped by satellite. In addition, periods of reduced thermal activity (e.g., 2022–May 2024) marked by NHI were in good agreement with information provided by independent sources. The accurate localization and mapping of high-temperature features, and the characterization of different eruptive phases, demonstrate that the NHI algorithm, through the GEE-App available online (<https://sites.google.com/view/nhi-tool/nhi-tool-for-volcanoes>), may support scientists also in the monitoring of frequently active volcanoes such as the Volcán de Fuego, providing information about changes of thermal volcanic activity that could precede future and more dangerous eruptions.

1. Introduction

The Volcán de Fuego (standing 3763 m a.s.l.) is a stratovolcano lying on the southern flank of the Fuego-Acatenango volcanic complex located along the WNW-trending central Guatemalan volcanic arc (Fig. 1) and is one of the most active volcanoes in the world (Chesner and Rose, 1984; Vallance et al., 2001; USGS, 2021). There have been more than 60 major eruptions (subplinian style) from this volcano in historical times (Vallance et al., 2001; Lyons and Waite, 2020). The current activity is part of an erupting phase which began in 1999 and characterized by an open-vent behaviour interspersed with infrequent paroxysmal eruptions (violent Vulcanian eruptions, VEI 2-3) lasting for 1–2 days that commonly produce pyroclastic flows (Vallance et al., 2001; Escobar, 2013; Lyons and Waite, 2011).

Volcanic products from direct (i.e. pyroclastic flows, tephra fall, lava flows) and indirect (e.g. lahars and debris avalanches) volcanic activity pose a serious threat to hundreds of thousands of inhabitants settle near the volcano (e.g. GVP, 2019a; Vallance et al., 2001). In recent years, intense eruptive events occurred in July–December 2017, February 2018 and June 2018 (GVP, 2019b). The most recent deadliest activity was recorded on 3 June 2018, when a series of pyroclastic flows were generated by the collapse of erupting columns that headed down on the SE flank of the volcano, travelling more than 11 km along different ravines. Most of the material descended through the Barranca (ravine) Las Lajas devastating the community of San Miguel Los Lotes, killing hundreds of people. Moreover, 332 people were officially reported missing (Flynn and Ramsey, 2020; Pardini et al., 2019 and references there in).

After the June 2018 events, the Volcán de Fuego's activity continued to be an interspersion of explosions generating pyroclastic flows and ash clouds practically on a daily basis, with the occasional emission of lava flows, and lahars triggered by

rain along different ravines. For details, the reader is referred to reports published by INSIVUMEH (Instituto Nacional de Sismología, Vulcanología, Meteorología e Hidrología; the scientific Guatemalan institution in charge of the volcano monitoring program (<https://insivumeh.gob.gt>) and the reports from the Global Volcanism Program (GVP) (<https://volcano.si.edu/volcano.cfm?vn=342090>).

INSIVUMEH maintains a 7-day 24-hour surveillance program on the active Guatemalan volcanoes. Sulphur dioxide, ash emission and thermal anomalies at Volcán de Fuego are monitored through satellite remote sensing data. Broadband and short period instruments perform the monitoring of the seismic activity. There is also an acoustic infrasound network and webcams to complement the ground-based monitoring of this volcano.

In this work, we investigate the eruptive activity of the Volcán de Fuego by satellite, exploiting the information provided by the operational NHI (Normalized Hotspot Indices) tool (Genzano et al., 2020). The latter enables the analysis of active volcanoes at global scale (i.e., over more than 1400 active volcanic areas) through the analysis of daytime L8/9 OLI (Operational Land Imager) and Sentinel 2 (S2) MSI (Multispectral Instrument) data. The study investigates the different periods of thermal activity (e.g., in terms of spatial extent and intensity level of volcanic thermal features), with the aim of inferring information about the eruptive behaviour of the Volcán de Fuego and evaluating the current state of thermal activity at the time of writing this paper. Hence, we present a long-term analysis (over more than 40 years of satellite observations) integrating results from Landsat 5 (L5) TM (Thematic Mapper), Landsat 7 (L7) ETM+ (Enhanced Thematic Mapper plus) data with the Landsat 8/9 (L8/9) ones, provided by the NHI tool. Moreover, the contribution of Sentinel-2 observations to the analysis of thermal anomalies at Volcán de Fuego also is analysed and discussed.

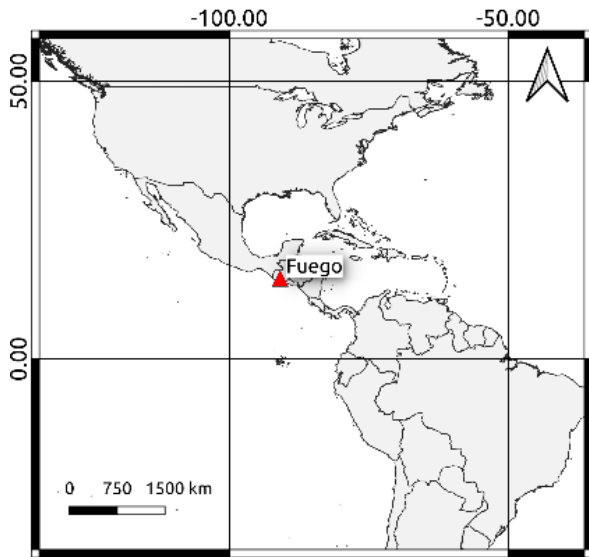


Fig. 1: Geographic location of Volcán de Fuego (Guatemala).

2. NHI Algorithm

The NHI algorithm uses two normalized hotspot indices to identify and map hot targets:

$$NHI_{SWIR} = \frac{L_{SWIR2} - L_{SWIR1}}{L_{SWIR2} + L_{SWIR1}} \quad (1)$$

$$NHI_{SWNIR} = \frac{L_{SWIR1} - L_{NIR}}{L_{SWIR1} + L_{NIR}} \quad (2)$$

L_{NIR} , L_{SWIR1} and L_{SWIR2} are the TOA (Top of the Atmosphere) radiances measured in the near infrared (NIR) (0.86 μm) and short-wave infrared (SWIR) bands (SWIR1, 1.6 μm ; SWIR2, 2.2 μm) of MSI and OLI sensors (providing infrared data at 20 m and 30 m spatial resolution). The NHI algorithm considers the pixels hot when they show positive values of one or both the aforementioned indices (Marchese et al., 2019). The algorithm was tested with success over different volcanic areas, showing high performance in the mapping of high-temperature features (e.g., lava flows), also through the analysis of daytime and nighttime ASTER (Advanced Thermal Emission and Reflection Radiometer) data acquired before the failure of the SWIR subsystem (Mazzeo et al., 2021). A preliminary analysis of some active volcanoes by means of TM and ETM+ data of the previous Landsat series was also performed (Genzano et al., 2020). The possibility of using the NHI algorithm to monitor short-term changes of thermal activity was then assessed by exploiting the Himawari 8 AHI (Advanced Himawari Imager) and GOES-R ABI (Advanced Baseline Imager) observations at very high temporal resolution (10 min) (Falconieri et al., 2022; Marchese et al., 2022).

2.1 NHI tool

Since early 2020, the NHI algorithm performs operationally under the GEE platform (Genzano et al., 2020), the catalogue of which is continuously updated at a rate of nearly 6000 scenes per day, with a latency of about 24 h from data acquisition (Google Earth Engine, 2024). The NHI tool, thanks to high computation resources and extended data archive of the GEE platform, allows users to analyze the volcanoes of interest without any authentication, through time series of the number of hot pixels,

total SWIR radiance and hotspot area (integrating information from L8/9 and S2 data), after a proper setting of some input parameters (Genzano et al. 2020). Moreover, the tool implements some additional spectral tests to minimize false positives and better map the extremely hot pixels (Genzano et al. 2020).

Information from the NHI tool was exploited with success to monitor several volcanoes such as Lateiki (Tonga), Mt. Etna (Italy), Kilauea and Mauna Loa (Hawaii), integrating information from satellite data at lower spatial/higher temporal resolution (e.g., Marchese et al., 2022; Plank et al., 2020; Genzano et al., 2023), revealing also the occurrence of an increasing phase of thermal activity at the Ambrym craters preceding the lava effusion of 15 December 2018 (Marchese et al., 2022).

The NHI system, i.e. the automated module of the tool, provides notifications about volcanic thermal anomalies detected over the previous 48 hours, whenever the web site is accessed (Marchese and Genzano, 2023).

3. Results

Fig. 2 displays the temporal trend of the hot pixels flagged the by NHI algorithm on TM (green dots), ETM+ (cyan dots) and OLI/OLI2 (violet dots) data at the same spatial resolution (30 m in the VNIR and SWIR bands) covering the Volcán de Fuego. The plot, displaying in grey the major periods of lava effusion from the Global Volcanism Program (GVP), shows the prevalence of a mid-low thermal activity during the period April 1985–August 1999. This is indicated by the low number of hot pixels flagged over the crater area, above 3700 m elevation. As an example, Fig. 3a shows the map generated from the L5-TM scene of 20 January 1996, revealing the presence of a small thermal anomaly of a low intensity level (see yellow pixels magnified in the figure inset). Indeed, a first increment in the number of hot pixels occurred on 25 April 1996, and was associated with image artefacts, as indicated by the analysis of TM data, while that recorded on 8 August 1999 was determined by a significant lava effusion occurring during a new eruptive period, which began on 21 May that year, after almost 12 years of very-low activity (GVP, 1999). The new eruptive period was characterized by Strombolian activity and sporadic paroxysmal events (e.g., Naismith et al., 2019). After that, the number of hot pixels decreased, in agreement with the absence of lava effusion, for almost two-year and a half, indicated by the bulletins and weekly reports of GVP. A new erupting phase began on 4 January 2002 consisting of Strombolian-type activity, while the lava flow effusion began by the end of the same month (GVP 2002a, 2002b). By mid-February, the volcanic activity increased and the lava flow was about 2-km-long (GVP, 2002c). This eruptive activity is marked by a minor peak in hot pixel number evident in Fig. 2. From June 2001 through August 2007, only data from L7-ETM+ were available (see cyan dots in Fig. 2). These data showed the presence of an extended thermal anomaly on 21 April 2003, i.e., during a documented period of incandescent avalanches (GVP, 2004). Afterwards, the thermal activity remained at a mid-low level, as indicated by the low number of hot pixels, mainly reflecting the thermal activity at the crater area. Since December 2012, a new increment of hot pixels occurred. On 26 January 2013, a lava flow extended up to about 2800 m elevation, as indicated by the NHI map of Fig. 3b. This new period of lava effusion is consistent with information provided by MODVOLC (Wright et al., 2022), indicating that lava flows were active near the summit region, and reporting the presence of thermal anomalies at Volcán de Fuego at least once per month during the period January 2011–March 2013. This information was also consistent with the information from the bulletins and weekly reports of the GVP, reporting an almost constant Strombolian activity, interspersed with explosions and lava

effusion. The temporal coverage of the investigated area increased since June 2013, when L8-OLI data became available. The analysis of those data, along with the L7-ETM+ ones, revealed the presence of smaller thermal anomalies ascribable to a mid-low level thermal activity recorded until February 2015, when a new increment in the number of hot pixels occurred. This increment preceded the peak of the time series, which was recorded on the L8-OLI scene of 7 September 2016. This peak was determined by an intense lava flow (see red pixels), extending up to about 2500 m elevation (Fig. 3c). After February 2018, both ETM+ and OLI data revealed the presence of less extended thermal anomalies, despite some increments in the hot pixel number (e.g., L7 ETM+ scene of 15 October 2021). To better characterize the recent Volcán de Fuego activity, we analysed the plot of total hotspot area (THA) provided by the NHI tool, integrating the Landsat 8/9 with the Sentinel-2 MSI observations (20 m spatial resolution), available since October 2015. Fig. 4 shows that the largest thermal anomaly (~ 0.5 km²) at the investigated volcano occurred on 6 September 2016. Thermal anomalies of a smaller spatial extent were then identified on satellite scenes of 25 January 2017 (S2-MSI; Fig. 5) and 1 February 2018 (L8-OLI), when a significant ash plume was also emitted (NASA, 2024). Increments in the THA were then

recorded in February 2021 and February 2022. Thermal anomalies of small size were mostly located over the crater area, as shown in Fig. 6 in reference to the minor activity reported on 29 March 2024 (e.g., Volcano Discovery, 2024).

By analysing the plot of total SWIR radiance (TSR), and taking into account the limitations affecting this parameter discussed in previous studies (e.g., Genzano et al., 2020; Planck et al., 2020), we inferred some information about the intensity of volcanic thermal emissions. The plot in Fig. 7 shows the temporal trend of the TSR retrieved from S2-MSI data (in black) and the total MIR radiance (TMR) derived from daytime MODIS observations (in red) (MODVOLC), referring to the period January 2017–May 2024. It is worth noting that the two parameters provided similar information about the major periods of lava effusion (e.g., 13 Feb 2021, 4 May 2023) and the decreasing trends of thermal volcanic activity. Results of a correlation analysis between the TMR and TSR shown in Fig. 8 corroborates the good agreement between results derived from daytime MODIS (MODVOLC) and MSI (NHI) data. Major differences in Fig. 7 characterized the peak of TMR recorded by MODVOLC on 11 July 2017, i.e., in absence of Sentinel-2 data covering the target area.

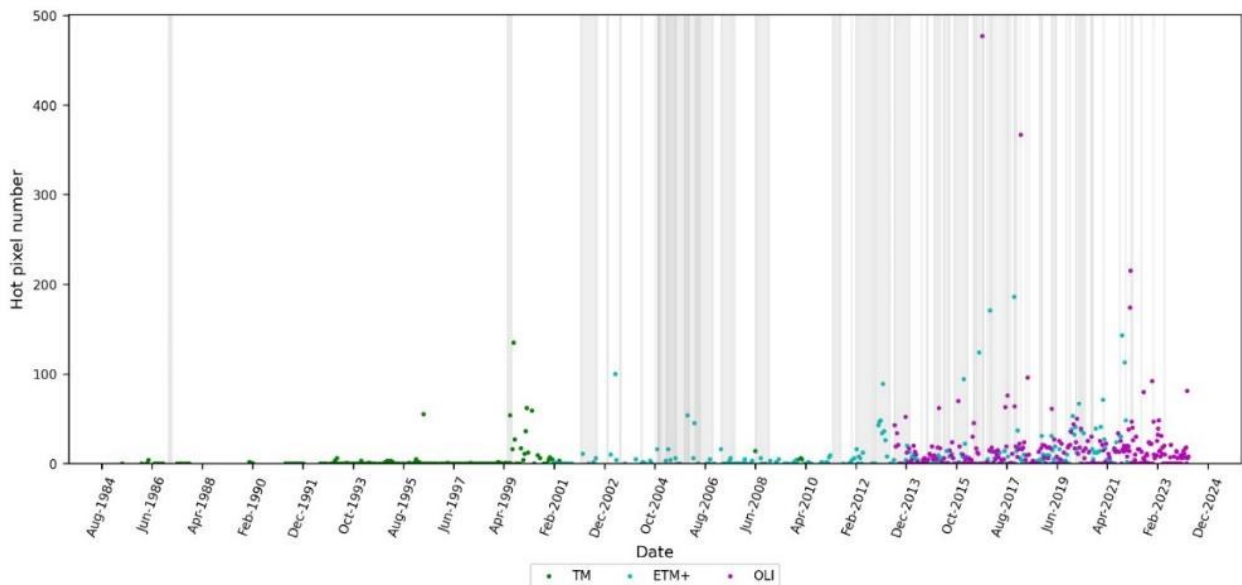


Fig. 2: Number of hot pixels flagged by NHI over Volcán de Fuego during the period April 1985–May 2024 from daytime L5-TM, L7-ETM+ and L8/9 OLI/OLI2 data. Grey bars indicate the periods of major lava effusion retrieved from the GVP bulletins.

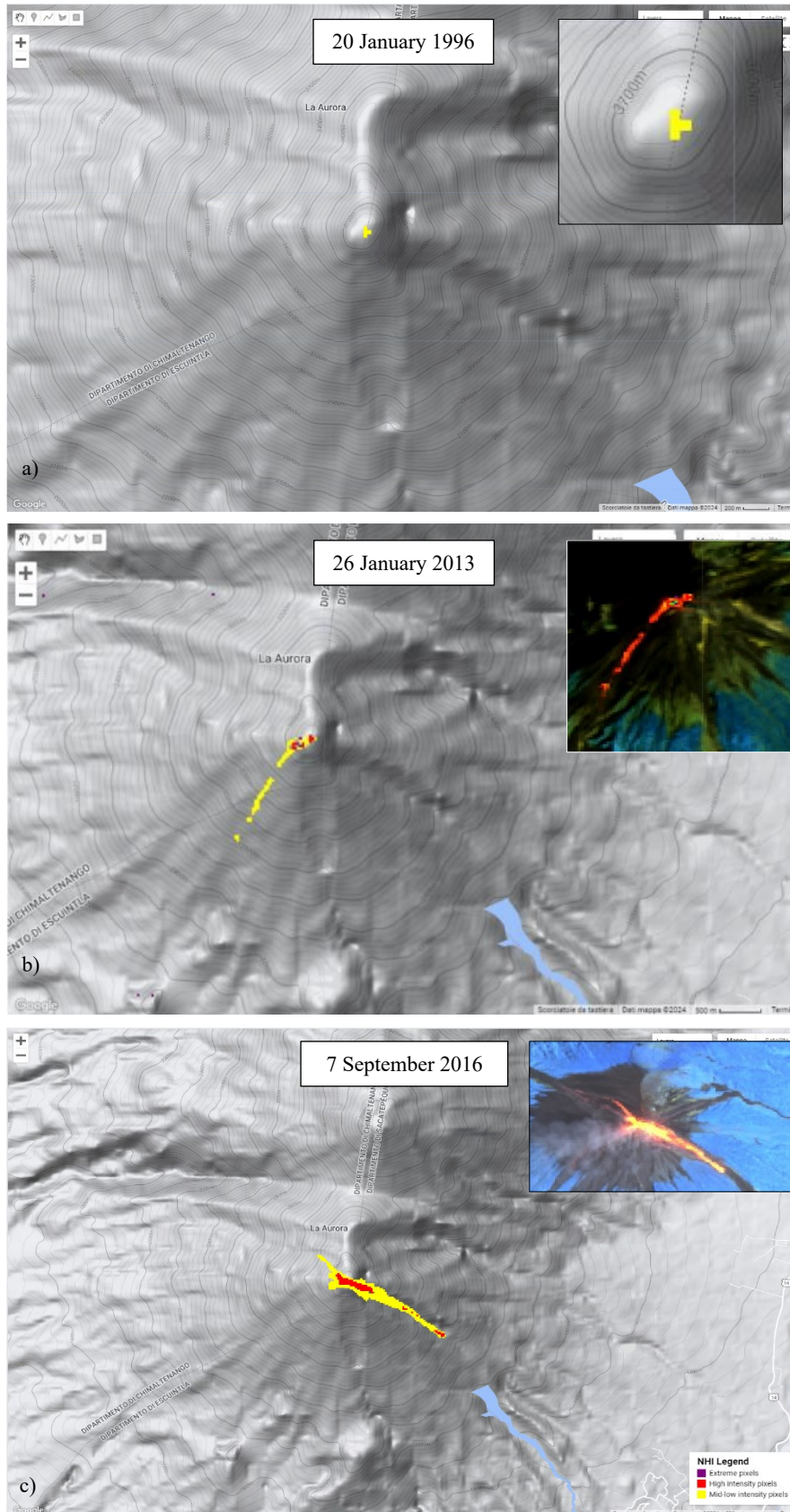


Fig. 3: NHI maps of the Volcán de Fuego generated from a) L5-TM scene of 20 January 1996; b) L7-ETM+ scene of 26 January 2013; c) L8-OLI scene of 7 September 2016. In yellow, pixels with values of $NHI_{SWIR} > 0$, in red those with $NHI_{SWNIR} > 0$, in violet the saturated pixels. In the inset of bottom panel, false colour image from bands B7 (SWIR2), B5 (SWIR1), B4 (NIR).

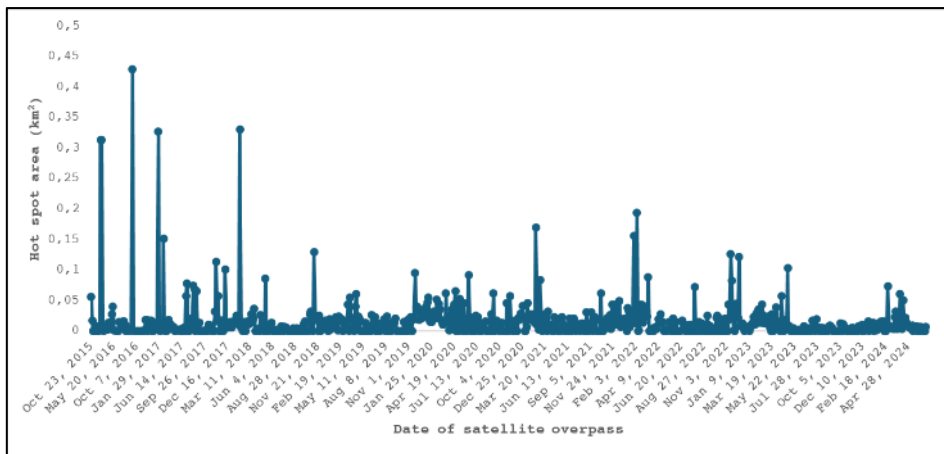


Fig. 4: Temporal trend of the hotspot area retrieved using the NHI tool over the period October 2015–May 2024.

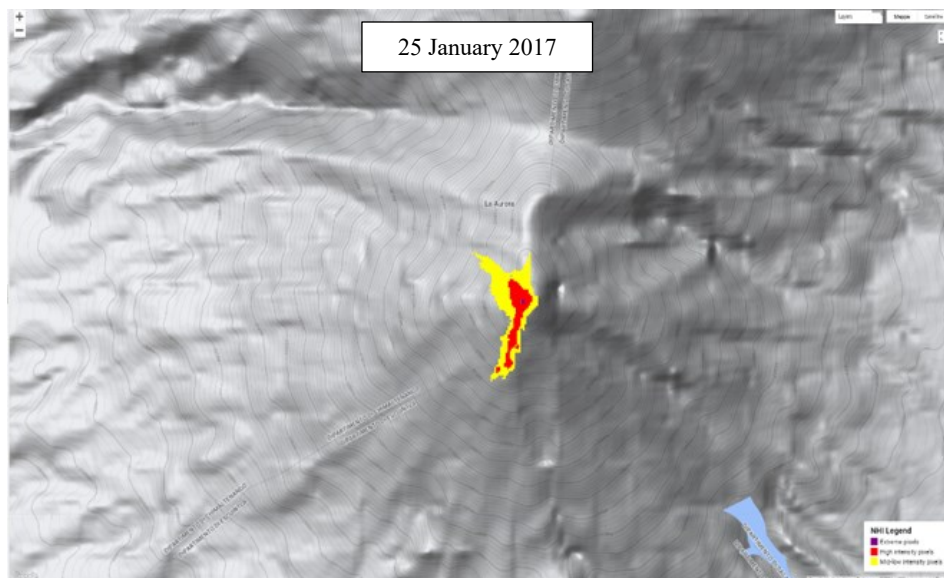


Fig. 5: Lava flow detected on S2-MSI scene of 25 January 2017. The different pixel colours have the same meaning as Fig. 3

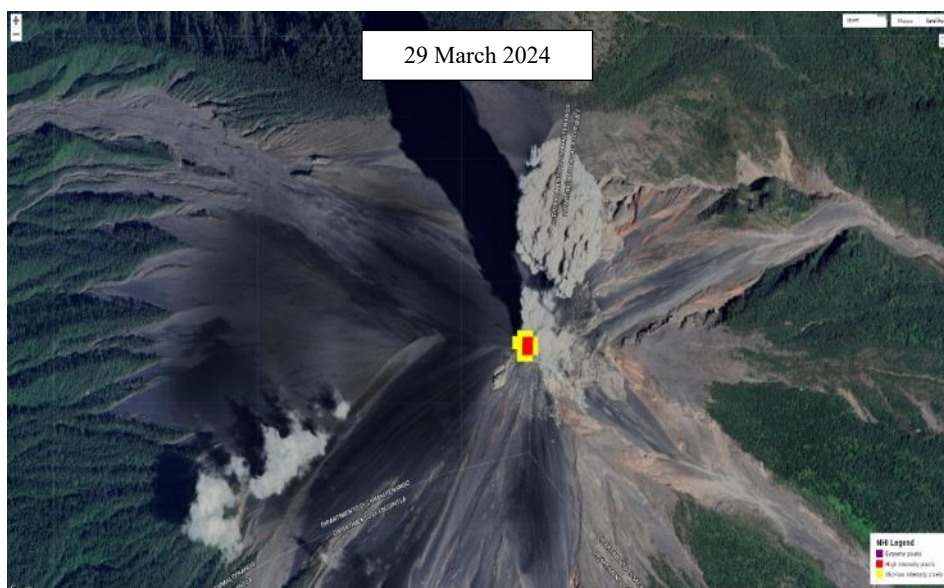


Fig. 6: Thermal anomaly detected on L9 OLI2 data of 29 March 2024. In background, a very high resolution image of the Volcán de Fuego available in GEE.

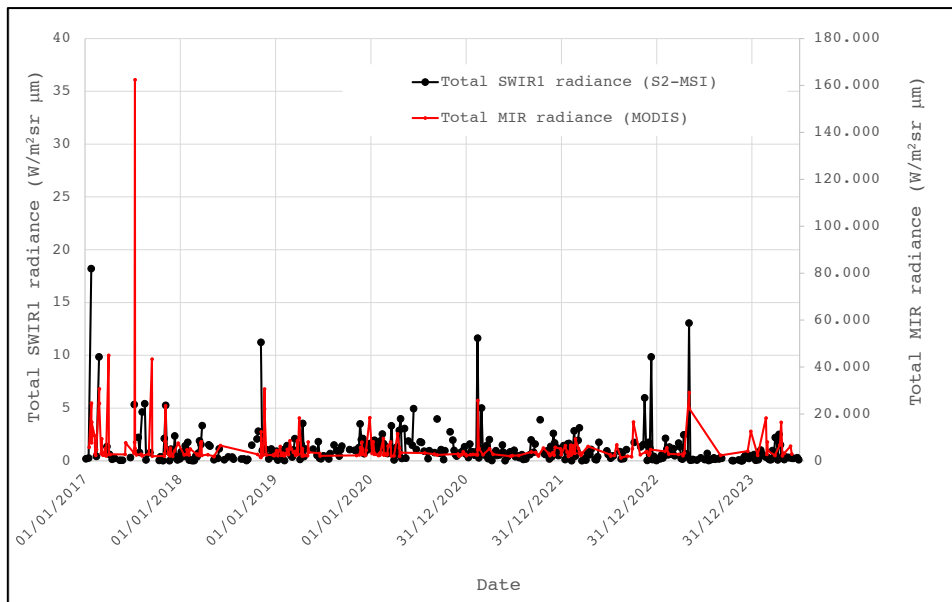


Fig. 7: Temporal trend of the total SWIR1 radiance (TSR) retrieved from S2-MSI data (NHI tool) and total MIR radiance (TMR) from daytime MODIS data (MODVOLC) of January 2017–May 2024.

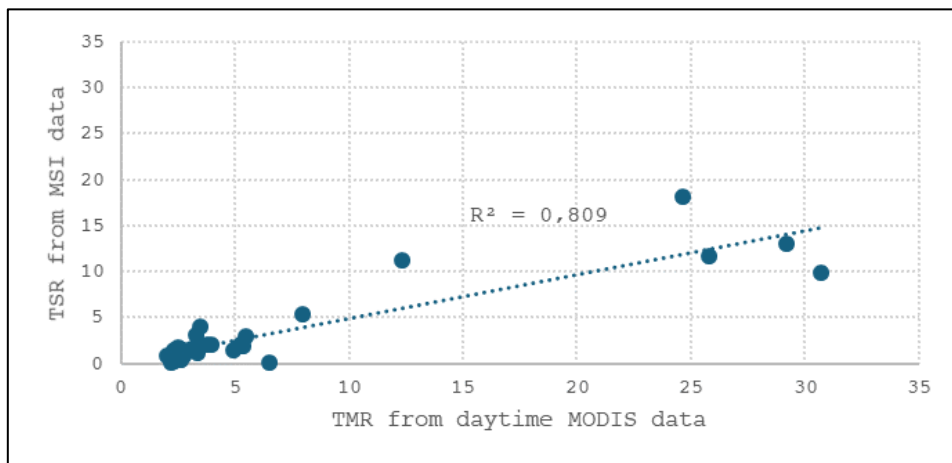


Fig. 8: Scatter plot between TMR (MODVOLC) and TSR (NHI) over the period January 2017–May 2024

4. Discussion and conclusions

In this work, we have presented the results of an extended time series analysis performed at the Volcán de Fuego, by integrating for the first time more than 40 years of daytime Landsat observations. By the temporal trend of the hot pixel number, we found that since 1986 and until April 1999 periods from minor to moderated thermal activity were prevalent (e.g., satellite scenes with less than 20 hot pixels represented about 74% of the time series). Afterwards, major periods of eruptive activity occurred (e.g., 2000–2003; 2012–2013; 2015–2018), as indicated by the significant increment in the hot pixel number mostly associated with lava effusions, in good agreement with information provided by independent sources. The NHI algorithm performed and efficient mapping of volcanic thermal features regardless of analysed Landsat data. Moreover, the striping effects affecting the L7-ETM+ scenes, due to the failure of the scan line corrector (SLC) in 2003 (<https://www.usgs.gov/faqs/what-landsat-7-etm-slc-data>), did not impact on results of this work, as indicated by the manual

inspection of satellite imagery. The integration of L8/9 OLI/OLI2 and S2-MSI observations, performed by the NHI tool, allowed us to characterize the recent Volcán de Fuego activity also from a quantitative point of view. Results appear consistent also with the information provided by MODVOLC (Figs. 7-8).

On the other hand, despite the combined revisit time of the Sentinel-2 and Landsat 8/9 satellites (see Marchese and Genzano, 2023) some major events (e.g., the second major eruption recorded in 2018; GVP, 2019c) remained undetected also because of cloudy conditions. Indeed, the temporal coverage of used data does not enable a continuous monitoring of the active volcanoes, unlike MODIS and VIIRS observations (e.g. Wright et al., 2004, Campus et al., 2022). Despite those limitations, daytime S2-MSI and L8/9 OLI/OLI2 data may provide, however, a unique contribution for the accurate localization and mapping of high-temperature features even of small spatial extent, as confirmed by results shown and discussed in this work. This study also confirms that the NHI algorithm may enable an effective

characterization of the different phases of thermal volcanic activity, contributing in a better understanding of eruptive dynamics. In this context, the NHI tool may highly support the monitoring of the Volcán de Fuego and other frequently active volcanoes, integrating the information from systems using satellite data at high-temporal/low-spatial resolution.

Acknowledgements

Sentinel-2 and Landsat 8/9 data used in this work were processed under the Google Earth Engine (GEE) platform. We thanks two anonymous reviewers for the suggestions devoted to improve the quality of the paper.

References

- Campus, A., Laiolo, M., Massimetti, F., Coppola, D., 2022. The transition from MODIS to VIIRS for global volcano thermal monitoring. *Sensors*, 22(5), 1713.
- Chesner, C.A., Rose Jr, W.I., 1984. Geochemistry and evolution of the Fuego volcanic complex, Guatemala. *Journal of Volcanology and Geothermal Research*, 21(1-2), 25-44.
- Escobar Wolf, R.P., 2013. Volcanic processes and human exposure as elements to build a risk model for Volcan de Fuego, Guatemala (Doctoral dissertation, Michigan Technological University).
- Falconieri A, Genzano N, Mazzeo G, Pergola N, Marchese F., 2022. First Implementation of a Normalized Hotspot Index on Himawari-8 and GOES-R Data for the Active Volcanoes Monitoring: Results and Future Developments. *Remote Sensing*, 14 (21), 5481, <https://doi.org/10.3390/rs14215481>
- Flynn, I.T., Ramsey, M.S., 2020. Pyroclastic density current hazard assessment and modeling uncertainties for Fuego Volcano, Guatemala. *Remote Sensing*, 12(17), 2790.
- Genzano, N., Pergola, N., Marchese F., 2020. A Google Earth Engine tool to investigate, map and monitor volcanic thermal anomalies at global scale by means of mid-high spatial resolution satellite data. *Remote Sensing*, 12(19), 3232.
- Genzano, N., Marchese, F., Plank, S., Pergola, N., 2023. Monitoring the Mauna Loa (Hawaii) eruption of November–December 2022 from space: Results from GOES-R, Sentinel-2 and Landsat-8/9 Observations. *International Journal of Applied Earth Observation and Geoinformation*, 122, 103388.
- Global Volcanism Program, 1999. Report on Fuego (Guatemala) (Wunderman, R., ed.). Bulletin of the Global Volcanism Network, 24:4. Smithsonian Institution. <https://doi.org/10.5479/si.GVP.BGVN199904-342090>
- Global Volcanism Program, 2002a. Report on Fuego (Guatemala) (Wunderman, R., ed.). Bulletin of the Global Volcanism Network, 9 January-15 January 2002. Smithsonian Institution. <https://volcano.si.edu/showreport.cfm?vvar=GVP.WVAR20020109-342090>
- Global Volcanism Program, 2002b. Report on Fuego (Guatemala) (Wunderman, R., ed.). Bulletin of the Global Volcanism Network, 23 January-29 January 2002. Smithsonian Institution. <https://volcano.si.edu/showreport.cfm?vvar=GVP.WVAR20020123-342090>
- Global Volcanism Program, 2002c. Report on Fuego (Guatemala) (Wunderman, R., ed.). Bulletin of the Global Volcanism Network, 13 February-19 February 2002. Smithsonian Institution. <https://volcano.si.edu/showreport.cfm?vvar=GVP.WVAR20020123-342090>
- Global Volcanism Program (GVP), 2004. Report on Fuego (Guatemala) (Wunderman, R., ed.). Bulletin of the Global Volcanism Network, 29:11. Smithsonian Institution. <https://doi.org/10.5479/si.GVP.BGVN200411-342090>
- Global Volcanism Program (GVP), 2019a. Report on Fuego (Guatemala) (Krippner, J.B., and Venzke, E., eds.). Bulletin of the Global Volcanism Network, 44:4. Smithsonian Institution. <https://doi.org/10.5479/si.GVP.BGVN201904-342090>.
- Global Volcanism Program (GVP), 2019b, Bulletin of the Global Volcanism Network, 43:2. Smithsonian Institution. <https://doi.org/10.5479/si.GVP.BGVN201802-342090>
- Global Volcanism Program (GVP), 2019c, Report on Fuego (Guatemala). In: Sennert, S K (ed.), Weekly Volcanic Activity Report, 30 May-5 June 2018. Smithsonian Institution and US Geological Survey.
- Google Earth Engine, 2024. A planetary-scale platform for Earth science data & analysis. <https://earthengine.google.com/>
- Marchese, F., Neri, M., Falconieri, A., Lacava, T., Mazzeo, G., Pergola, N., Tramutoli, V., 2018. The Contribution of Multi-Sensor Infrared Satellite Observations to Monitor Mt. Etna (Italy) Activity during May to August 2016. *Remote Sensing*, 10, 1948.
- Marchese, F., Genzano, N., Neri, M., Falconieri, A., Mazzeo, G., Pergola, N., 2019. A Multi-Channel Algorithm for Mapping Volcanic Thermal Anomalies by Means of Sentinel-2 MSI and Landsat-8 OLI Data. *Remote Sensing*, 11(23), 2876. doi.org/10.3390/rs11232876.
- Marchese, F., Neri, M., Behncke, B., Genzano, N., 2020. Main morpho-structural changes and eruptions of Etna in 2016-2019 captured by satellite observations. In EGU 2020, General Assembly Conference Abstracts, doi: [10.5194/egusphere-egu2020-13909](https://doi.org/10.5194/egusphere-egu2020-13909)
- Marchese, F., Coppola, D., Falconieri, A., Genzano, N., Pergola, N., 2022. Investigating Phases of Thermal Unrest at Ambrym (Vanuatu) Volcano through the Normalized Hot Spot Indices Tool and the Integration with the MIROVA System. *Remote Sensing*, 14, 3136. <https://doi.org/10.3390/rs14133136>
- Marchese, F., Genzano, N., 2023. Global volcano monitoring through the Normalized Hotspot Indices (NHI) system. *Journal of the Geological Society*, 180 (1), jgs2022-014, <https://doi.org/10.1144/jgs2022-014>
- Mazzeo, G., Ramsey, M.S., Marchese, F., Genzano, N., Pergola, N., 2021. Implementation of the NHI (Normalized Hot Spot Indices) Algorithm on Infrared ASTER Data: Results and Future Perspectives. *Sensors*, 21, 1538. doi.org/10.3390/s21041538
- National Aeronautics and Space Administration (NASA), 2024. Earth Observatory. <https://earthobservatory.nasa.gov/images/91671/fuego-erupt>
- Naismith, A. K., Watson, I. M., Escobar-Wolf, R., Chigna, G., Thomas, H., Coppola, D., Chun, C., 2019) Eruption frequency patterns through time for the current (1999–2018) activity cycle at Volcán de Fuego derived from remote sensing data: Evidence for an accelerating cycle of explosive paroxysms and

potential implications of eruptive activity. *Journal of Volcanology and Geothermal Research*, 371, 206-219.

Lyons, J.J., Waite, G.P., 2011. Dynamics of explosive volcanism at Fuego volcano imaged with very long period seismicity. *Journal of Geophysical Research: Solid Earth*, 116(B9).

Pardini, F., Queißer, M., Naismith, A., Watson, I.M., Clarisse, L., Burton, M.R., 2019. Initial constraints on triggering mechanisms of the eruption of Fuego volcano (Guatemala) from 3 June 2018 using IASI satellite data. *Journal of Volcanology and Geothermal Research*, 376, 54-61.

Plank, S., Marchese, F., Genzano, N., Nolde, M., Martinis, S. (2020). The short life of the volcanic island New Late'iki (Tonga) analyzed by multi-sensor remote sensing data. *Scientific reports*, 10(1), 1-15. doi.org/10.1038/s41598-020-79261-7

Vallance, J.W., Schilling, S.P., Matias, O., Rose Jr, W.I., Howell, M.M., 2001. Volcano hazards at fuego and acatenango, guatemala (No. 2001-431). US Geological Survey.

Wright, R., Flynn, L.P., Garbeil, H., Harris, A.J., Pilger, E., 2004. MODVOLC: near-real-time thermal monitoring of global volcanism. *Journal of Volcanology and Geothermal Research*, 135(1-2), 29-49.

Volcano Discovery, 2024. Fuego volcano (South-Central Guatemala) - Smithsonian / USGS Weekly Volcanic Activity Report for 20 March-26 March 2024 (Continuing Activity). <https://www.volcanodiscovery.com/it/fuego/news/237689/Fuego-volcano-South-Central-Guatemala-Smithsonian-USGS-Weekly-Volcanic-Activity-Report-for-20-March-.html>

USGS, 2001. Volcano Hazards at Fuego and Acatenango, Guatemala <https://pubs.usgs.gov/of/2001/0431/pdf/of2001-0431.pdf>